Variation of Laser Absorption with Plasma Scale Length in Long-Scale-Length Plasmas

M. J. Herbst, J. Grun, J. Gardner, J. A. Stamper, F. C. Young, S. P. Obenschain, E. A. McLean, and B. H. Ripin
U. S. Naval Research Laboratory, Washington, D.C. 20375
(Received 11 August 1983)

A short-pulse, high-intensity Nd-laser beam interacts with preformed plasmas of variable scale length. At the longest scale length, absorption is limited by backscatter, despite increased collisional absorption.

PACS numbers: 52.50.Jm, 52.35.Py, 52.40.Db

The achievement of high-gain laser fusion depends upon the efficient absorption of laser light in the underdense plasma surrounding the fuel pellet. Furthermore, the absorption *mechanisms* are important: A premium is placed upon collisional absorption, which preferentially produces thermal particle distributions. Other absorption processes tend to produce energetic particles, which may penetrate the pellet shell and preheat the fuel, thereby impeding the compression required for high gain.

The absorption processes which dominate in small plasmas are likely to be entirely different from those which dominate in large plasmas, because the effectiveness of each process varies differently with the density-inhomogeneity scale length $L_n \equiv |n/\nabla n|$. For example, resonance absorption,[1] shown to dominate in small plasmas,[2] becomes *less* important with longer L_n, while collisional absorption[3] becomes *more* important. Unfortunately, parametric instabilities[4] are also predicted to become more effective in larger plasmas; these can either degrade absorption efficiency by scattering incident laser light or degrade absorption quality by generating energetic particles. Experimental studies of this changing role of different absorption processes are important because high-gain pellets will be surrounded by much larger plasmas than in recent experiments. In this work, we describe the first long-scale-length experiments with controlled variations of plasma scale length. As the scale length increases, backscatter limits the absorption efficiency despite increased collisional absorption.

To study high-intensity laser absorption in long-scale-length plasmas, we use a novel configuration of our two-beam, Nd ($\lambda_0 = 1.054$ μm) laser. One beam generates long-scale-length background plasmas; it has a 4-nsec duration and irradiates a large area (90% of the energy is within a diameter $d_{90} \simeq 1080$ μm), giving a peak irradiance of about 6×10^{12} W/cm^2 at the surface of the polystyrene film target. To produce higher irradiances for absorption studies, we tightly focus our second beam (50% of the energy is within $d_{50} \simeq 90$ μm) along the central axes of the plasmas produced by the first beam. The second beam is synchronous with the peak of the first beam, and its duration is reduced to 300 psec to minimize hydrodynamic perturbations to the background plasmas. Vacuum intensities (averaged within d_{50}) in the short pulse vary between 10^{14} and 10^{15} W/cm^2 for incident energies E between 4 and 40 J. Intensities in the plasma may be altered by self-focusing[5]; therefore, incident energies are quoted. Initially, the two beams have orthogonal linear polarizations, but passage through a quarter-wave plate produces opposite circular polarizations at the target, and converts circularly polarized backscatter to linear polarization before detection.

Plasma characterization.—To vary the scale length, the background beam is apertured to reduce d_{90} from 1080 μm to either 640 or 360 μm; hereafter, we refer to these as the long-, medium-, and short-scale-length background plasmas, respectively. Density profiles measured by third-harmonic interferometry are compared in Fig. 1 with predictions of our hydrodynamics code,[6] a two-dimensional (2D), cylindrical model with collisional absorption and classical thermal conduction. As a result of experimental uncertainty in the target position, the data have been shifted in z for the best fit with the calculation. Therefore, the data only confirm code-predicted scale lengths for densities $n < n_c/4$. At $n = n_c/10$, for example, L_n/λ_0 varies from 200 to 400 as the spot size is increased. The code predicts that overdense-plasma scale lengths do not vary at these spot sizes: L_n/λ_0 at critical density is calculated to be near 45 for all three background conditions. Plasma velocity profiles, important for Brillouin scattering,[4] are not shown but are

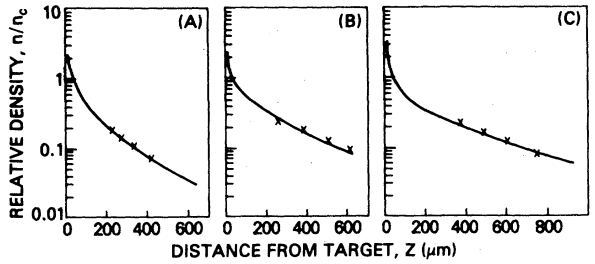

FIG. 1. On-axis profiles of density n relative to critical density n_c. Code results (curve) and interferometric results (points) are shown for (a) short-, (b) medium-, and (c) long-scale-length background plasmas.

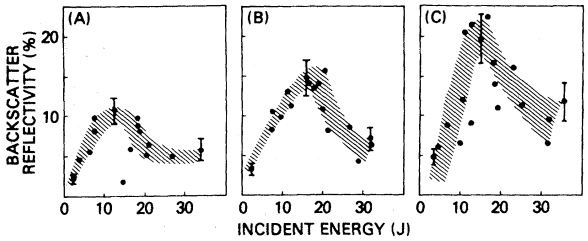

FIG. 2. Backscatter reflectivities for (a) short-, (b) medium-, and (c) long-scale-length background plasmas.

directly related to the density profiles by the hydrodynamics. The background plasmas have nearly the same peak coronal temperature because the apertured beam has nearly constant irradiance; the code predicts a variation from 415 eV in the short-scale-length plasma to 525 eV in the long-scale-length plasma.

Additional plasma heating results from irradiation by the high-intensity beam. This is monitored by measuring thermal x-ray emission with two subnanosecond scintillator photodiodes filtered to look at 1.0–1.5- and 2.0–2.8-keV x-rays, respectively.[7] Ratios of these detector signals imply time-averaged x-ray temperatures during the short pulse which are factors of 1.1 to 1.8 higher than the peak background temperatures for short-pulse energies of 4 to 40 J. These x-ray temperature increases are consistent with estimates from free-bound continuum spectra predicted by the 2D code. Similar increases are observed in the calculated, peak coronal temperatures.

This localized heating can cause density perturbations. The creation of density channels along the laser axis in the underdense plasma is experimentally inferred from time-integrated images of second-harmonic emission obtained for $E \gtrsim 15$ J.[7] These data also provide evidence for self-focusing of the beam in these channels. For $E < 15$ J, the images infrequently indicate density channels and almost never suggest self-focusing.

The 2D code also predicts density perturbations which strengthen with increasing incident energy. As E increases from 5 to 25 J, on-axis density minima form earlier in time and over greater radial extent. The maximum depth $\Delta n/n$ increases from about 5% at 5 J to about 15% at 25 J. These may be lower bounds on $\Delta n/n$, however, since the code does not include beam refraction by these perturbations (i.e., self-focusing). The code also predicts axial perturbations; a shock propagates down the density gradient into the underdense plasma, perhaps as a transient response to the increased mass-ablation rate of the higher-intensity beam. With increased incident energy, this shock strengthens and occurs at earlier times.

Scattered light and absorption.—Backscatter through the incident $f/6.7$ lens is observed with both time-resolving and time-integrating detectors. A photodiode with 700-psec rise time distinguishes short-pulse backscatter from the lower level of long-pulse backscatter. We quote energy reflectivities of the short pulse, since this detector cannot resolve within the short pulse. Backscattered energy is monitored with use of two calorimeters, one for each polarization. The short-pulse backscatter is preferentially polarized with the polarization of the high-intensity beam, unlike the unpolarized backscatter of the background beam. Backscatter reflectivities, as shown in Fig. 2, increase with incident energy for $E \lesssim 15$ J, but decrease at higher energies.

Properties of the backscatter are consistent with production by stimulated Brillouin scattering.[4] Backscattered light has the polarization of the incident beam. For $E \lesssim 15$ J, the reflectivity R increases with incident energy and the rate of this increase becomes greater with increased scale length. While R decreases for $E > 15$ J, this may be due to the strong plasma perturbations at higher incident energies. The axial shock predicted by the code, for example, could reduce Brillouin backscatter since it produces an abrupt change in the plasma velocity profile. This apparent backscatter reduction could also be due to an increased angular spread of backscatter at higher incident energies, since scattered light just outside the incident lens is not monitored.

As shown in Fig. 3(a), light scattered outside of the incident lens is measured with five subnanosecond diodes: four are deployed on one side of the specular angle (12°) in the plane of incidence of the laser, and the fifth samples light on the other side. If we assume symmetry about the specular direction, we can infer the total amount of scattered light outside the incident lens. In contrast to backscatter, the amount of this light decreases with increasing background scale length. The reflectivity S integrated over the angular distribution varies with incident energy as shown in Figs. 3(b)–3(d).

The observations of scattered light outside the lens are consistent with the hypothesis that this is nonabsorbed light that has been specularly reflected from the critical-density surface. The decrease of S at longer scale length can be explained by increased collisional absorption, which reduces the penetration of ingoing light to critical density and of outgoing reflected light to detectors. The increase of S with incident energy can be explained by increased plasma heating, which reduces collisional absorption.

Experimental absorption fractions $\eta = 1 - R - S$ are close to code predictions for collisional absorption alone. (For this comparison, the incident energy in the code is reduced by the observed backscatter.) As shown in Fig. 4, experimental values of η are consistent with or slightly greater than calculated values, but by no more than 10% of the incident energy. This slight gap has at least three possible explanations: (1) With the limited number of detectors, some scattered light may be missed, causing an overestimate of η; (2) the code may underestimate the collisional absorption since it gives slightly higher x-ray temperatures than are measured; and (3) absorption mechanisms other than collisional absorption may be operative. None of these alternatives significantly affects the inferred absorption fractions, although explanation (3) raises concern about generation of suprathermal particles by the additional absorption mechanism(s).[7]

Although the absorption fractions seem mainly due to a combination of collisional absorption and backscatter, the mechanism that limits η changes with the background scale length. We restrict ourselves to $E \lesssim 15$ J, where effects of plasma perturbations are believed to be minimal. For the short scale length, we find low levels of backscatter and at least an equal amount of scattered light at other angles. If the latter is specular scatter, we infer that η is limited primarily by the inefficiency of collisional absorption in the short-scale-length plasma; even without backscatter, collisional absorption could not greatly increase. In contrast, the long-scale-length case exhibits larger backscatter and little scattered light at other angles; we infer that collisional absorption is very efficient, and that backscatter now limits the absorption fraction.

These are the first measurements of absorption in variable-scale-length plasmas, and the results have important implications for laser fusion. Plasmas surrounding high-gain pellets will differ from those of the present experiment:

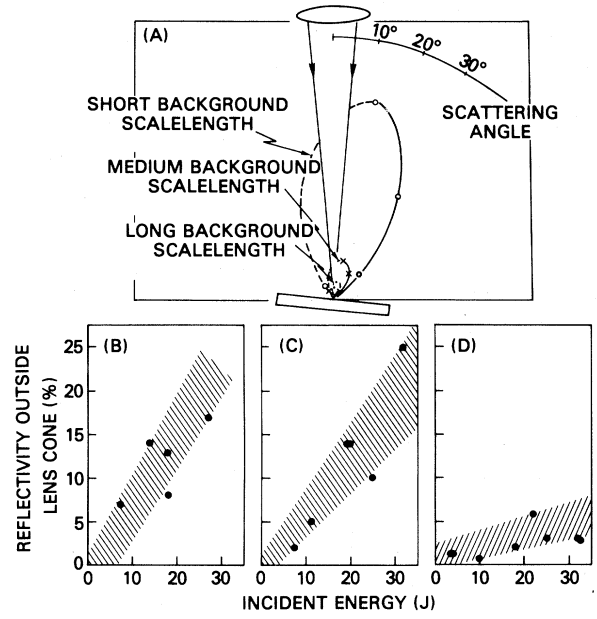

FIG. 3. (a) Angular distributions of light scattered outside the lens cone for $E \simeq 10$ J. Reflectivities, integrated over angles, for (b) short-, (c) medium-, and (d) long-scale-length background plasmas.

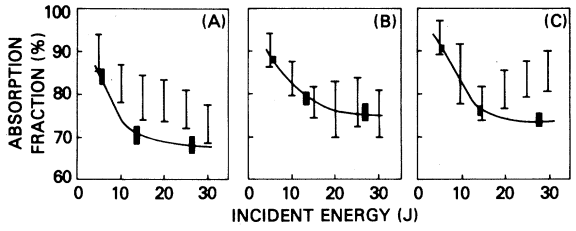

FIG. 4. Comparison between experimental absorption fractions (narrow bars) and calculated collisional absorption (solid curve with wide bars to indicate uncertainties) for (a) short-, (b) medium-, and (c) long-scale-length background plasmas.

Scale lengths L are expected to be longer by factors of 5 or more and temperatures T are predicted to be greater by factors of 2 or more. Collisional absorption,[3] which scales with $L/T^{3/2}$, would then be at least as efficient in a high-gain system as in the present experiment. Levels of backscatter, on the other hand, will depend upon ion-wave damping rates and instability noise levels,[4] which may differ from those of the present experiment. Nonetheless, the observed increase of backscatter with scale length suggests that backscatter may severely reduce absorption efficiencies at the much longer scale lengths of high-gain systems. Hopefully, proposed mechanisms,[8] such as shorter laser wavelength or wider laser bandwidth, will be sufficient to control backscatter.

Although the new experimental approach described here allows study of longer scale lengths with a given laser energy and enables one to vary the scale length in a controlled manner, it has limitations. First, one must allow for possible effects on the results due to the perturbations of the background plasma. Second, the limited diameter of the high-intensity beam may prevent adequate simulation of some plasma instabilities (e.g., Brillouin sidescatter) that require a larger transverse interaction region.

The authors wish to acknowledge valuable conversations with Dr. S. E. Bodner and Dr. R. H. Lehmberg. We also appreciate the technical assistance of M. Fink, K. Kearney, J. Kosakowski, N. Nocerino, E. Turbyfill, and B. Sands. This work was supported by the U. S. Department of Energy and the U. S. Office of Naval Research. One of us (J.G.) was employed at Mission Research Corp., Alexandria, Va., while this work was being done.

[1]V. L. Ginzburg, *The Propagation of Electromagnetic Waves in Plasmas* (Pergamon, Oxford, 1970).

[2]K. Estabrook and W. L. Kruer, Phys. Rev. Lett. 40, 42 (1978), and references contained therein.

[3]T. W. Johnston and J. M. Dawson, Phys. Fluids 16, 722 (1973).

[4]C. S. Liu, in *Advances in Plasma Physics*, edited by A. Simon and W. B. Thompson (Wiley, New York, 1976), Vol. 6, pp. 121 ff, and references contained therein.

[5]J. A. Stamper *et al.*, U. S. Naval Research Laboratories Memorandum Report No. 5173, 1983 (unpublished).

[6]J. Gardner *et al.*, U. S. Naval Research Laboratories Memorandum Report No. 5170, 1983 (to be published).

[7]F. C. Young *et al.*, U. S. Naval Research Laboratories Memorandum Report No. 5174, 1983 (unpublished).

[8]S. E. Bodner, J. Fus. Energy 1, 211 (1981), and references contained therein.